Determination of Absolute Configuration in Molecules with Chiral Axes by Vibrational Circular Dichroism: A C 2 Symmetric Annelated Heptathiophene and a D 2 Symmetric Dimer of 1,1‘−...

ARTICLE *in* THE JOURNAL OF PHYSICAL CHEMISTRY A · OCTOBER 2003

Impact Factor: 2.69 · DOI: 10.1021/jp030307v

Determination of Absolute Configuration in Molecules with Chiral Axes by Vibrational Circular Dichroism: A C_2-Symmetric Annelated Heptathiophene and a D_2-Symmetric Dimer of 1,1′-Binaphthyl

Teresa B. Freedman,*,† Xiaolin Cao,† Andrzej Rajca,*,‡ Hua Wang,‡ and Laurence A. Nafie*,†

Department of Chemistry, Syracuse University, Syracuse, New York 13244-4100, and Department of Chemistry, University of Nebraska, Lincoln, Nebraska 68588-0304

Received: March 6, 2003; In Final Form: June 5, 2003

The absolute configurations of two large molecules that possess chiral axes, but no chiral centers, have been determined by vibrational circular dichroism (VCD): an annelated heptathiophene (a helical molecule with C_2-symmetry) and a π-conjugated chiral derivative of *o*-tetraphenylene (a D_2-symmetric dimer of 1,1′-binaphthyl). In both cases, the size of these molecules exceeds the current limit of published structures for which VCD has been used to determine the absolute configuration. In the case of the annelated heptathiophene, 3 different elements, and 11 total (7 S atoms, 2 Si atoms, and 2 Cl or Br atoms), beyond the second row in the periodic table are included in the calculated structure. In the case of the tetraphenylene molecule, a total of 40 C atoms constitutes the hydrocarbon structure, which is a new upper limit for the number of atoms beyond H for which VCD has been calculated for the determination of absolute configuration. The excellent agreement between observed IR and VCD spectra and spectra calculated at the density functional theory (B3LYP/6-31G*) level for these molecules provides definitive determination of their absolute configurations and establishes a new regime of molecular size and elemental variety for which accurate comparisons of VCD calculations to experiment can be conducted.

Introduction

Vibrational circular dichroism (VCD),[1] which is the differential interaction of a chiral molecule with left and right circularly polarized infrared (IR) radiation during vibrational excitation, has proven to be a powerful method for the identification of absolute configuration and solution conformation.[2−7] The technique entails comparison of observed spectra with calculations for a specified enantiomer and conformation at the density functional theory (DFT) level. In this paper, we focus on two large chiral molecules that possess chiral axes, but no chiral centers: the annelated heptathiophene ($C_{22}H_{18}Br_2S_7Si_2$), **1**, which is a helical C_2-symmetric molecule,[8] and the π-conjugated chiral derivative of *o*-tetraphenylene ($C_{40}H_{24}$), **2**, which is a D_2-symmetric dimer of 1,1′-binaphthyl.[9,10] These two molecules, and a third molecule with a C_2-chiral axis (gossypol, $C_{30}H_{30}O_8$), which is reported separately,[11] are the largest investigated thus far in full experimental and computational detail with VCD. DFT VCD calculations for alanine decapeptides have been reported recently to model peptide helices, but without direct comparison to experiment.[12] Although a VCD study of a small molecule that contained bromine ((+)-1-bromo-2-methylbutane) has been reported,[13] the heptathiophene, **1**, is the first molecule to our knowledge with multiple atomic centers beyond the second row in the periodic table, and it is the first molecule with two fourth-row atoms, for which VCD intensities have been calculated, thus establishing new ground in the size and elemental richness in molecules for which VCD can be used for the determination of the absolute configuration.

Heptathiophene, **1**, may be viewed as a fragment of an unusual $(C_2S)_n$ carbon−sulfur helix that provides a novel motif for connectivity in oligothiophenes, which are an important class of molecules studied as organic materials.[14] Although the helical geometry of **1** is analogous to that of hexahelicene,[8] the formally cross-conjugated C═C bonds in **1** create an interesting π-system. Determination of the absolute configuration for (−)-**1** and (+)-**2** is relevant to their asymmetric syntheses via axially symmetric dilithiated biaryls, including asymmetric induction of axial chirality by (−)-sparteine and correlation with axially chiral 1,1′-binaphthyl.[9,10]

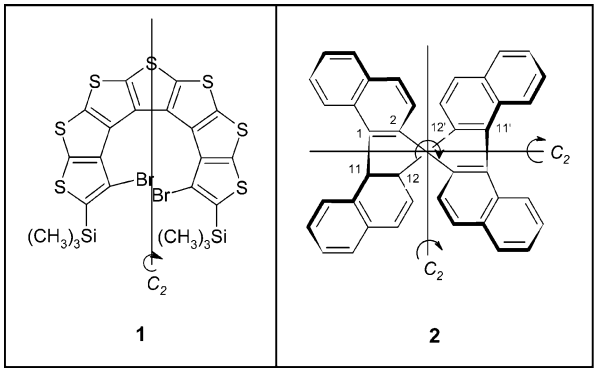

X-ray crystallographic determination of absolute configurations for **1** has been thwarted by the difficulty in growing suitable crystals of a single enantiomer, and X-ray determination with a synchnotron source was also unsuccessful.[15] The X-ray structure for **2** has been obtained;[9] however, the data were not complete enough to allow for determination of the absolute configuration. For both **1** and **2,** electronic circular dichroism

* Authors to whom correspondence should be addressed. E-mail: tbfreedm@syr.edu, lnafie@syr.edu.
† Syracuse University.
‡ University of Nebraska.

10.1021/jp030307v CCC: $25.00
Published on Web 09/06/2003

(CD) spectra have been measured, but conjugation of the chromophores precludes application of the exciton coupling model to the UV−visible CD spectra for determination of absolute configurations. Recently, Ahlrichs and co-workers demonstrated a qualitative agreement between the time-dependent DFT (TDDFT) calculations and experimental UV−visible CD spectra of helicenes;[16] TDDFT calculations have not been obtained for **1** or **2**. The present DFT/VCD studies provide an alternative, and inherently richer and simpler, approach for establishing absolute configurations of large-sized molecules with axially chiral π-conjugated systems.

Recently, we performed VCD measurements and ab initio intensity calculations for molecules with heavier atomic centers, using both transition-metal complexes (+)-tris(ethylenediaminato)cobalt(III)[17] and Zn(II) with sparteine and chloride ligands.[18] In one study,[18] strong VCD enhancement, without accompanying IR enhancement, was observed for two transition-metal complexes that possess low-lying electronic transitions, namely Co(II) and Ni(II) sparteine, and these enhancements are currently beyond the range of reliable VCD intensity calculations. The present study is the first attempt to calculate the VCD spectrum of a molecule with multiple non-transition-metal third- and fourth-row elements.

Materials and Methods

Modification of the racemic synthesis of **1**[8] using (−)-sparteine provided (−)-**1** with 20% enantiomeric excess (ee).[10,19] Fractional crystallization using $CDCl_3$/MeOH gave (−)-**1** with increased enantiomeric excesses. Synthesis of (+)-**2** was described previously.[9] Enantiomeric excesses were determined using ^{1}H NMR spectroscopy (Bruker, 500 MHz, $CDCl_3$) with chiral shift reagents. Ag(fod) and ytterbium tris[3-heptafluoropropylhydroxymethylene)−(+)-camphorate] were added until baseline separation between enantiomers in selected resonances was attained.[9,10] For **1**, ^{1}H resonances of the trimethylsilyl groups were complicated by incompletely resolved ^{29}Si−^{1}H two-bond couplings from 4.7% abundance of ^{29}Si. Integrations were obtained directly from resolved spectra or by numerical lineshape fitting using NUTS software. Optical rotations were measured at 589 nm with Autopol III (Rudolph Research) at ambient temperature.

Samples of (−)-**1** (~3 mg, 84% ± 5% ee) and (+)-**2** (~9 mg, 84% ± 5% ee; ~7 mg, 67% ± 5% ee) were dissolved in $CDCl_3$ (100 μL) and then placed in a BaF_2 cell with a path length of 94.1 μm. IR and VCD spectra were measured on a modified Chiral*IR* VCD spectrometer[20,21] (BioTools) at a resolution of 4 cm^{-1}, with the instrument being optimized at 1400 cm^{-1}. Acquisition times for the sample and solvent were 18 h for **1** and 9 h for **2**. A long acquisition time was required to reduce the VCD noise for **1**, because of the small amount of sample available. Corresponding solvent spectra were used for both IR and VCD baselines.

Calculations of the optimized geometry of a selected enantiomer of each molecule were performed at the DFT level (6-31G(d) or larger basis sets, B3LYP functional) with Gaussian 98[22] on either a Pentium IV personal computer (PC) (1.5 GHz processor, 1 GB memory) or on up to eight processors on the HP N-4000 complex at the University of Kentucky High Performance Computing Center. For **1** (51 atoms, 597 basis functions, 1322 primitive Gaussians for 6-31G(d)), 25 optimization steps required 31 computer processing unit (CPU) h on the eight-processor HP cluster. For **2** (64 atoms, 648 basis functions, 1216 primitive Gaussians for 6-31G(d)), seven steps of optimization on the PC required 59 CPU h. Vibrational frequencies and IR and VCD intensities were calculated at the same level on the eight-processor HP N-4000 cluster (52 CPU h for **1** and 110 CPU h for **2**), with Gaussian 98, utilizing the magnetic-field perturbation method with gauge-invariant atomic orbitals.[23] The frequency/intensity calculations could not be completed on the PC. For **1**, the calculations were also performed with Cl substituents in place of the Br substituents on the helix, and for **2**, calculations were also performed with 6-311G(d), 6-31+G(d), and 6-31G(d′p′) basis sets on the HP Superdome Cluster at the University of Kentucky High Performance Computing Center.

For comparison to experiment, the calculated frequencies were scaled by 0.97, and the calculated intensities were converted to Lorentzian bands with half-widths of 6 cm^{-1} for **1** and 2 or 4 cm^{-1} for **2**.

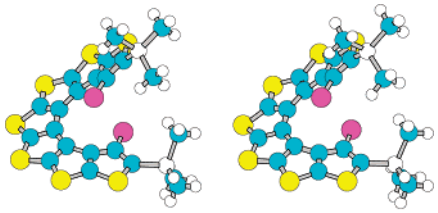

Figure 1. Comparison of the optimized structure of (*R*)-**1** (DFT/6-31G* basis, B3LYP functional) with the structure determined by X-ray crystallography.

Results and Discussion

The calculated optimized structure of (*R*)-**1** is compared to the X-ray structure for the racemate[8] (drawn for the *R*-enantiomer) in Figure 1. The molecule crystallizes with one chloroform molecule statistically disordered over two positions.[8] Adequate crystals of enantiomerically pure **1** have not been able to be obtained so far, precluding determination of absolute configuration by X-ray crystallography. In the racemic crystal, the inner nine-C-atom helix climbs 2.92 Å and turns in-plane by 260°, with quite similar calculated values. The Br···Br distance is 3.90 Å in the crystal and 3.82 Å in the calculated structure, and the average of the C−Br distances is 1.89 Å in the crystal and 1.90 Å in the calculation. For the chloro analogue, the calculated Cl···Cl distance is 3.76 Å and the average C−Cl bond length is 1.75 Å. The experimental IR and VCD spectra of (−)-**1** are shown in Figure 2, where the low-frequency limit at 930 cm^{-1} results from strong $CDCl_3$ solvent absorbance. The calculated spectra for both the Br and Cl analogues in the left-handed helical *R*-configuration are compared to experiment in Figure 3, where the experimental intensities have been adjusted to 100% ee and converted to molar absorptivity units (10^3 cm^2/mol). For this helical molecule, almost every band in the experimental IR and VCD spectra correlates with a band of identical sign and similar intensity in the calculated spectra. The excellent agreement between experiment and calculation provides a definitive assignment of (−)-**1** to the *R*-configuration left-handed helix. Substitution of chlorine for bromine has a very minor effect on the calculated structure or spectra of the helix.

The calculated optimized structure of (*R*)-**2** is shown in Figure 4, along with labeling of the chiral axes of the binaphthyl 1,1′- and 2,2′-linkages. For convenience, the enantiomer is identified by the axis associated with the 1,1′-linkage. The calculated and X-ray structures[9] have very similar geometries, with approximate D_2 symmetry and with planar naphthalene rings. The torsion angles in the center ring are −70.4° (X-ray) and −72.3° (DFT)

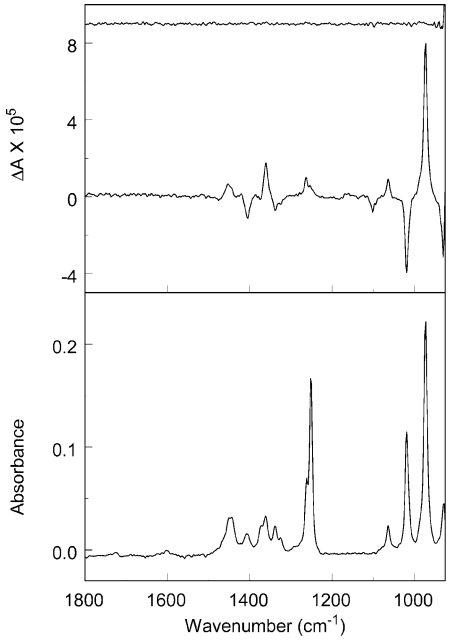

Figure 2. Observed IR (lower frame) and VCD (upper frame) spectra of (−)-**1**, 84% ± 5% ee, ~3 mg/100 μL $CDCl_3$, 94.1-μm BaF_2 cell, 18 h collection. Uppermost trace is the VCD noise.

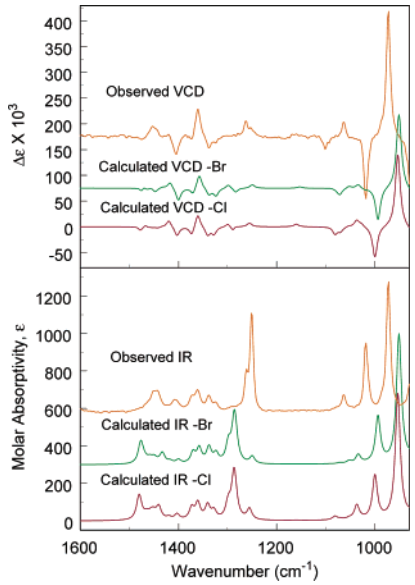

Figure 3. Comparison of IR (lower frame) and VCD (upper frame) spectra of (−)-**1** with calculation for the *R*-enantiomer with Br and Cl substituents. Spectra are offset for clarity.

for the C2−C1−C11−C12 dihedral angle and 68.2° (X-ray) and 65.9° (DFT) for the C11−C12−C12′-C11′ dihedral angle. The experimental IR and VCD spectra of (+)-**2** are presented in Figure 5. The two samples provided to us yielded very similar spectra, with relative VCD intensities that were consistent with their difference in enantiomeric excess. The spectrum shown is for (+)-**2** with 84% ee. The calculated spectrum of (*R*)-**2** (using the 6-31G(d) basis set) is compared to the experimental spectrum of (+)-**2** in Figure 6, with all spectra given in molar absorptivity units (10^3 cm^2/mol) and the experimental spectra adjusted to 100% ee. There is superb band-to-band correlation between the observed and calculated spectra, permitting a definitive assignment to (*R*)−(+)-**2**. In Figure 6, the calculated spectra have been plotted both with a smaller half-width (2 cm^{-1}), to amplify the visual correlation, and a 4-cm^{-1} half-width, which is closer to the experimental value. We note that the absolute intensity

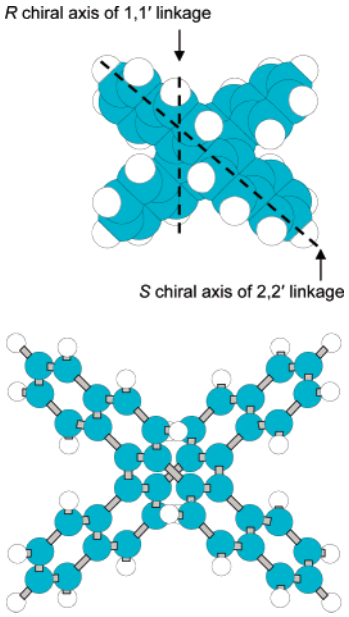

Figure 4. Space-filling and ball-and-stick representations of the calculated structure of (*R*)-**2**, showing labeling of chiral axes for the 1,1′- and 2,2′-linkages.

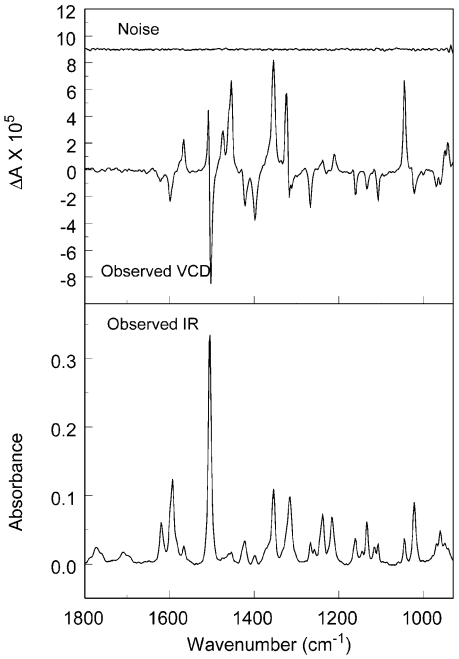

Figure 5. Observed IR (lower frame) and VCD (upper frame) spectra of (+)-**2**, 84% ± 5% ee, ~9 mg/100 μL $CDCl_3$, 94.1-μm BaF_2 cell, 9 h collection. Uppermost trace is the VCD noise.

correlations between experiment and calculation are dependent on the accuracies of the enantiomeric excess determinations and the experimental concentrations, which are somewhat uncertain for the small masses of samples available for both **1** and **2,** and on the volatility of the solvent. For **1**, the relative intensity correlation between observed and calculated IR and VCD spectra is excellent. For **2**, the observed and calculated anisotropy ratios ($\Delta\epsilon/\epsilon$) are similar, but the calculated IR and VCD are both smaller than the observed values, with a larger deviation for the VCD, which suggests that the experimental concentration may have been >9 mg/100 μL, because of solvent evaporation, or that the sample enantiomeric excess percentage was at the upper limit or higher than the range determined by NMR (84% ± 5% ee).

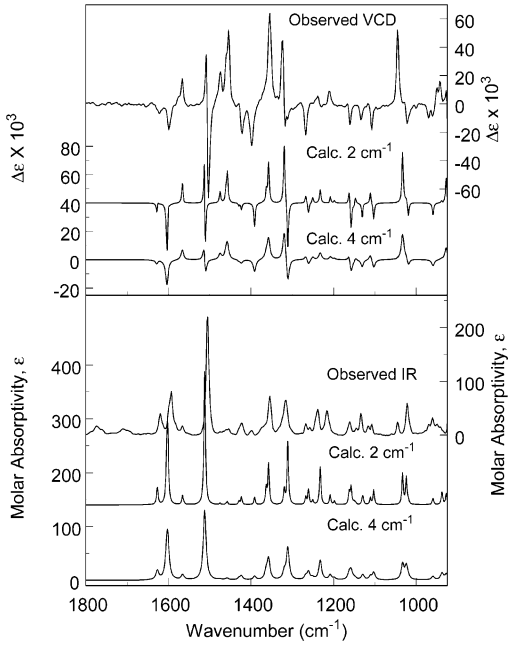

Figure 6. Comparison of IR (lower frame) and VCD (upper frame) spectra of (+)-**2** (upper traces, right axes) with calculated spectra for the *R*-enantiomer with a 6-31G(d) basis set (lower traces, left axes).

For the C_2-symmetric molecule, **1**, the normal modes are A and B species described by in-phase and out-of-phase motions on opposite positions of the helical molecule. The bands with the largest VCD intensity (Figure 3) correspond to ring motions that involve C−S stretch accompanied by C−Si stretch (∼930 (−, B); ∼972 (+, A); ∼1020 (−, B)) and the ring C−C stretches that also include motion of the C atom bonded to the Si atom (for example, ∼1369 (+, A); ∼1373 (−, B); ∼1404 (−, B); ∼1450 (+, A)). These modes are also intense in the IR spectrum. Modes that involve deformations of the methyl groups on opposite ends of the helix are too weakly coupled to generate significant frequency splittings, and the VCD intensities that are generated by the A and B pairs cancel for the methyl deformations. In the calculated spectrum, the methyl rocks contribute to an intense VCD couplet near 850 cm^{-1}, which is beyond the limit of the experimental measurement for the solvent used. Overall, the VCD intensities do not exhibit anomalously large anisotropy ratios ($>5 \times 10^{-4}$) that are attributable to the helical arrangement of the atoms in **1**. However, the calculation reveals a few VCD bands with weak IR intensity that have large anisotropy ratios ($\sim 1 \times 10^{-3}-2 \times 10^{-3}$). Examples of such include the weak positive VCD band observed at ∼1150 cm^{-1} and the negative band at ∼1100 cm^{-1}, which correspond to calculated modes that involve extended motion of the inner carbon helix and asymmetric distortion of C_4S rings that can produce large magnetic dipole contributions from angular charge circulation. Shifts in frequency between the observed and calculated spectra may arise either from the quality of the DFT functionals (particularly for Si, S, and Br atoms), from the basis set used, or from solvent interactions.

Although electronic CD spectra of **1** have been measured, but not calculated, calculations of the electronic CD of hexahelicene, substituted hexahelicenes and heptahelicene with TDDFT methods have been compared to experiment.[16] The TDDFT calculations for the electronic CD of heptahelicene (50 excitations) and our DFT calculations of the VCD spectra of heptathiophene **1** (147 vibrations) used a similar number of heavy atoms and basis functions. However, the TDDFT calculations required diffuse basis functions (for Rydberg excitations), which are not necessary for the VCD calculation; vibronic effects were neglected in the TDDFT formulation and implementation. The qualitative fit to experiment for the electronic CD of the helicenes varied with the number of rings and the nature and presence of substituents in the terminal rings. In general, the calculations were sufficient for identification of an absolute configuration; however, some disagreements with experiment, in regard to sign and relative intensity, were observed. In contrast, almost one-to-one correspondence in sign and relative intensity between experiment and calculation of the IR and VCD spectra is observed for the heptathiophene (−)-(*R*)-**1**.

For the D_2-symmetric molecule, **2**, the totally symmetric vibrations of the A species are IR inactive, whereas the modes of B_1, B_2, and B_3 symmetry species are both IR and VCD active and entail motions in-phase or out-of-phase, relative to the three orthogonal C_2-axes. The coupled motions among the four naphthalene moieties are split sufficiently for individual VCD features to be observed. No overall unexpectedly large anisotropy ratios for the VCD bands are observed for **2**, which implies that any π-conjugation present does not provide an extended pathway for vibrationally induced electron-charge flow. Again, the calculations show a few extremely weak modes with local charge circulation that have large anisotropy ratios, but such modes are obscured by more-intense bands. The agreement between the calculations (for an isolated gas-phase molecule) and both the solution spectra and the X-ray geometry reflects the weak interaction with $CDCl_3$ solvent and weak interactions in the crystal, as might be expected for a hydrocarbon. The comparison between the observed and calculated spectra for 2- and 4-cm^{-1} bandwidths (Figure 6) reveal that some of the differences between observed and calculated intensities result from the cancellation of adjacent positive and negative bands, which may be more similar, in regard to frequency, in the calculation than in experiment. To assess whether the intensity differences are due to the size and nature of the basis set, the calculation was repeated for several other basis sets. The addition of p-orbitals for the H atoms (6-31G(d′p′) basis) or of diffuse functions (6-31+G(d) basis) had only minor effects on the VCD intensities (not shown). The larger 6-311G(d) basis set produced slight increases in VCD intensity and some improvement in agreement with experiment, particularly at ∼1400 cm^{-1}, as shown in Figure 7.

Most applications of VCD to the determination of absolute configuration and solution conformation that have been published to date have focused on small-to-medium-sized organic molecules that have zero or, at most, one element beyond the second row.[11,13,24−26] Recently, we have explored the possibility of extending this limit significantly by conducting VCD measurements and ab initio calculations of the first transition-metal complexes,[17,18] which include open-shell Co(II) and Ni(II) sparteine complexes, for which the VCD intensities exhibit an approximate 10-fold increase in magnitude, compared to the Zn(II) sparteine complex, whereas the three IR spectra are almost identical.

Thus, it was with some considerable interest that we undertook the study of the chiral heptathiophene molecule featured here that possesses seven S atoms and two Si atoms from the third row and two Br atoms from the fourth row. The high level of correlation between the measured and calculated VCD and IR spectra demonstrates that there are no significant sources of unusual intensity enhancement in this molecule. This is particularly significant for the comparison of the calculated VCD for the bromine to chlorine versions of this molecule, cf.

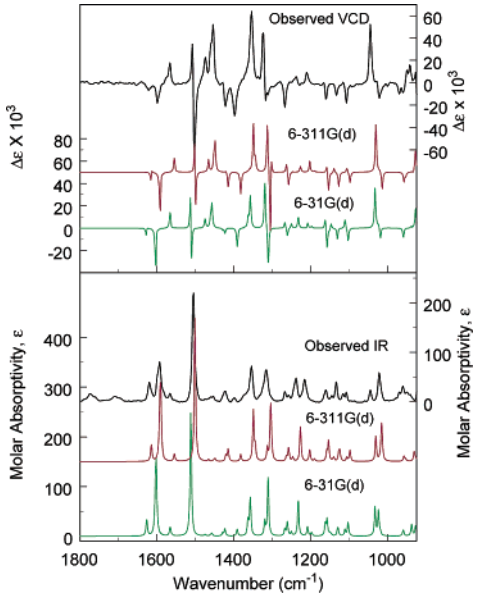

Figure 7. Comparison of IR (lower frame) and VCD (upper frame) spectra of (+)-**2** (upper traces, right axes) with calculated spectra for the *R*-enantiomer with 6-311G(d) and 6-31G(d) basis sets (lower traces, left axes, half-width of 2 cm^{-1}).

Figure 3, which shows no significant differences in intensity between these two structures. We are able to conclude that the basis functions used for the fourth-row element bromine lead to no significant changes in calculated intensity, compared to that of chlorine, and, because of the close agreement between experimental and calculated VCD intensities for the bromine molecule, current theoretical formalism can be extended to compounds with at least this fourth-row element.

Conclusions

For these two large, conformationally rigid molecules with chiral axes (the annelated heptathiophene ($C_{22}H_{18}Br_2S_7Si_2$), **1**, and the π-conjugated chiral derivative of *o*-tetraphenylene ($C_{40}H_{24}$), **2**), density functional theory calculations at the B3LYP/6-31G* level, which utilize the magnetic-field perturbation method of calculating VCD intensities and gauge-invariant atomic orbitals, provide almost perfect band-to-band agreement with the experimental spectra. The samples were as small as 3 mg, and the quantitative agreement is within the uncertainty of the concentrations and optical purity. The superb agreement easily provides definitive assignment of the absolute configurations. The left-handed helical *R*-configuration for the levorotatory enantiomer, (−)-**1**, is analogous to that found in helicenes. From the synthesis standpoint, the *R*-configurations for (−)-**1** and (+)-**2** are consistent with the selectivity of (−)-sparteine toward (*R*)-dilithiated biaryls and the transfer of configuration of the starting 2,2′-dibromo-1,1′-binaphthyl, respectively. The configuration determined for **2** confirms the configurational stability of the reactive intermediates, including 2,2′-dilithiobinaphthyl, under the experimental conditions used. This study extends the range of size and elemental richness of molecules for which reliable VCD calculations can be performed.

Acknowledgment. This research was supported by the National Science Foundation (through Grant No. CHE-0107241 to A.R. and Grant No. CHE-0111402 to L.A.N. and T.B.F.) and the National Institutes of Health (through Grant No. GM63148 to L.A.N. and T.B.F.). We acknowledge support for the computations from the National Computational Science Alliance (to T.B.F.), using the University of Kentucky HP N-4000 Complex and HP Superdome Complex.

References and Notes

(1) Nafie, L. A.; Freedman, T. B. In *Circular Dichroism: Principles and Applications, Second Edition*; Berova, N., Nakanishi, K., Woody, W., Eds.; Wiley: New York, 2000; pp 97−131.

(2) Nafie, L. A.; Freedman, T. B. In *Infrared and Raman Spectroscopy of Biological Materials*; Yan, B., Gremlish, H.-U., Eds.; Marcel Dekker: New York, 2001; pp 15−54.

(3) Polavarapu, P. L.; Zhao, C. *Fresenius' J. Anal. Chem.* **2000**, *366*, 727−734.

(4) Stephens, P. J.; Devlin, F. J. *Chirality* **2000**, *12*, 172−179.

(5) Solladié-Cavallo, A.; Sedy, O.; Salisova, M.; Biba, M.; Welch, C. J.; Nafie, L. A.; Freedman, T. B. *Tetrahedron: Asymmetry* **2001**, *12*, 2703−2707.

(6) Solladié-Cavallo, A.; Balaz, M.; Salisova, M.; Suteu, C.; Nafie, L. A.; Cao, X.; Freedman, T. B. *Tetrahedron: Asymmetry* **2001**, *12*, 2605−2611.

(7) Solladié-Cavallo, A.; Marsol, C.; Pescitelli, G.; Di Bari, L.; Salvadori, P.; Huang, X.; Fujioka, N.; Berova, N.; Cao, X.; Freedman, T. B.; Nafie, L. A. *Eur. J. Org. Chem.* **2002**, 1788−1796.

(8) Rajca, A.; Wang, H.; Pink, M.; Rajca, S. *Angew. Chem., Int. Ed.* **2000**, *39*, 4481−4483.

(9) Rajca, A.; Safronov, A.; Rajca, S.; Wongsriratanakul, J. *J. Am. Chem. Soc.* **2000**, *122*, 3351−3357.

(10) Rajca, A.; Wang, H.; Bolshov, P.; Rajca, S. *Tetrahedron* **2001**, *57*, 3725−3735.

(11) Freedman, T. B.; Cao, X.; Oliveira, R. V.; Cass, Q. B.; Nafie, L. A. *Chirality* **2003**, *15*, 196−200.

(12) Bour, P.; Kubelka, J.; Keiderling, T. A. *Biopolymers* **2002**, *65*, 45−59.

(13) Wang, F.; Polavarapu, P. L.; Lebon, F.; Longhi, G.; Abbate, S.; Catellani, M. *J. Phys. Chem. A* **2002**, *106*, 12365−12369.

(14) Fichou, D. *J. Mater. Chem.* **2000**, *10*, 571−588.

(15) Pink, M., personal communication.

(16) Furche, F.; Ahlrichs, R.; Wachsmann, C.; Weber, E.; Sobanski, A.; Vötgle, F.; Grimme, S. *J. Am. Chem. Soc.* **2000**, *122*, 1717−1724.

(17) Freedman, T. B.; Cao, X.; Young, D. A.; Nafie, L. A. *J. Phys. Chem. A* **2002**, *106*, 3560−3565.

(18) He, Y.; Cao, X.; Nafie, L. A.; Freedman, T. B. *J. Am. Chem. Soc.* **2001**, *123*, 11320−11321.

(19) Details of the asymmetric synthesis of **1** will be published elsewhere by A. Rajca and H. Wang.

(20) Dukor, R. K.; Nafie, L. A. In *Encyclopedia of Analytical Chemistry: Instrumentation and Applications*; Meyers, R. E., Ed.; Wiley: Chichester, U.K., 2000; pp 662−676.

(21) Nafie, L. A. *Appl. Spectrosc.* **2000**, *54*, 1634−1645.

(22) Frisch, M. J.; Trucks, G. W.; Schlegel, H. B.; Scuseria, G. E.; Robb, M. A.; Cheeseman, J. R.; Zakrzewski, V. G.; Montgomery, J. A., Jr.; Stratmann, R. E.; Burant, J. C.; Dapprich, S.; Millam, J. M.; Daniels, A. D.; Kudin, K. N.; Strain, M. C.; Farkas, O.; Tomasi, J.; Barone, V.; Cossi, M.; Cammi, R.; Mennucci, B.; Pomelli, C.; Adamo, C.; Clifford, S.; Ochterski, J.; Petersson, G. A.; Ayala, P. Y.; Cui, Q.; Morokuma, K.; Malick, D. K.; Rabuck, A. D.; Raghavachari, K.; Foresman, J. B.; Cioslowski, J.; Ortiz, J. V.; Stefanov, B. B.; Liu, G.; Liashenko, A.; Piskorz, P.; Komaromi, I.; Gomperts, R.; Martin, R. L.; Fox, D. J.; Keith, T.; Al-Laham, M. A.; Peng, C. Y.; Nanayakkara, A.; Gonzalez, C.; Challacombe, M.; Gill, P. M. W.; Johnson, B. G.; Chen, W.; Wong, M. W.; Andres, J. L.; Head-Gordon, M.; Replogle, E. S.; Pople, J. A. *Gaussian 98*, revision A.9; Gaussian, Inc.: Pittsburgh, PA, 1998.

(23) Cheeseman, J. R.; Frisch, M. J.; Devlin, F. J.; Stephens, P. J. *Chem. Phys. Lett.* **1996**, *252*, 211−220.

(24) Aamouche, A.; Devlin, F. J.; Stephens, P. J. *J. Am. Chem. Soc.* **2000**, *122*, 2346−2354.

(25) Stephens, P. J.; Aamouche, A.; Devlin, F. J. *J. Org. Chem.* **2001**, *66*, 3671−3677.

(26) Freedman, T. B.; Dukor, R. K.; van Hoof, P. J. C. M.; Kellenbach, E. R.; Nafie, L. A. *Helv. Chim. Acta* **2002**, *85*, 1160−1165.